ELSEVIER

Polymer 42 (2001) 2077–2083

polymer

www.elsevier.nl/locate/polymer

Miscibility of poly(ethyl oxazoline)/poly(4-vinylphenol) blends as investigated by the high-resolution solid-state ^{13}C NMR

J. Wang[a], M.K. Cheung[b], Y. Mi[a,*]

[a]*Department of Chemical Engineering, The Hong Kong University of Science and Technology, Clear Water Bay, Kowloon, Hong Kong, People's Republic of China*

[b]*Department of Applied Biology & Chemical Technology, The Hong Kong Polytechnic University, Hung Hom, Kowloon, Hong Kong, People's Republic of China*

Received 4 April 2000; received in revised form 1 June 2000; accepted 12 June 2000

Abstract

The miscibility of poly(ethyl oxazoline) (PEOx) and poly(4-vinylphenol) (PVPh) blends were investigated by differential scanning calorimeter (DSC), Fourier-transform infrared spectroscopy (FTIR), and high-resolution solid-state nuclear magnetic resonance (NMR) spectroscopy. It was found that PEOx was miscible with PVPh as shown by the existence of single composition-dependent glass transition temperature (T_g) in the whole composition range. FTIR results revealed strong hydrogen bonding between the carbonyl groups of PEOx and the hydroxyl groups of PVPh. ^{13}C cross-polarization (CP)/magic angle spinning (MAS)/dipolar decoupling (DD) spectra of the blends showed significant chemical shift changes, which support the FTIR results. The proton spin–lattice relaxation times in both the laboratory frame, T_1(H), and the rotating frame, $T_{1\rho}$(H), were studied as a function of blend composition, and blends gave values longer than pure polymers. The T_1(H) results are in good agreement with the thermal analysis; i.e. the blends are completely homogenous on the scale of 30–40 nm. The $T_{1\rho}$(H) results further indicate that the blends were homogenous on the scale of 2–3 nm.

Keywords: Poly(ethyl oxazoline); Poly(4-vinylphenol); Polymer blends

1. Introduction

Over the past few decades, polymer blends have been of great interest to materials scientists because of the improved or modified properties over the individual constituent polymers. For example, blending has the effect of toughening and strengthening for engineering applications. It was also reported that polymer blending can lead to functional polymeric materials that have desired electrical conductivity and magnetic properties [1,2]. Since the physical properties of polymer blends are strongly influenced by blending conditions and processes that, in turn, affect the level of mixing of the blends, there is a growing interest in studying miscibility and phase behavior of polymer blends.

Various techniques have been employed to investigate miscibility of polymer blends, such as microscopy, thermal analysis, dynamic mechanical analysis, dielectric measurements, diffraction, and spectroscopy [3–6]. Differential scanning calorimetry (DSC) is one of the most widely used techniques for evaluating miscibility on a scale of 100–300 Å, in terms of cooperative motion of polymer segments around the glass transition temperature (T_g) [6,7]. Infrared (IR) adsorption is sensitive to the local environment of the oscillating dipoles, and has proven to be a powerful technique for investigating intermolecular interactions [8].

Nuclear magnetic resonance (NMR) spectroscopy can evaluate characteristic molecular motions. NMR parameters are sensitive to the effects of spin diffusion and can monitor variations among discrete structural entities [9–11]. The ^{13}C chemical shifts and line shapes in cross-polarization (CP)/magic angle spinning (MAS)/dipolar decoupling (DD) spectra identify chemical environments of carbon in the blends, and changes usually reflect mixing between blend components [12–14].

Certain proton relaxation times are sensitive to the domain size of polymer blends through the process of spin diffusion. Two useful proton spin-relaxation times that can be obtained from ^{13}C solid-state NMR are the spin–lattice relaxation time in the laboratory frame T_1(H), and in the

* Corresponding author.

PII: S0032-3861(00)00502-4

rotating frame, $T_{1\rho}$(H), respectively. Proton spin diffusion is not a physical movement of protons, but is rather a transfer of spin energy by successive energy-conserving spin flips between a more magnetized region and a less magnetized region [9,15–17]. The spin diffusion process may be modeled as Fickian diffusion. Inter-domain spin diffusion in polymer blends may be detected directly by ^{1}H CRAMPS (combination of rotation and multiple pulse spectroscopy), ^{1}H WISE (wide-line separation), and Goldman–Shen experiments, or indirectly by its effects on the proton relaxation times T_1(H) and $T_{1\rho}$(H), [18,19]. T_1(H) is measured at specific protonated carbon sites by first having the protons go through inversion-recovery before cross polarization to ^{13}C. $T_{1\rho}$(H) is measured by monitoring the cross-polarized ^{13}C intensity after a variable proton spin-lock time. The ^{13}C intensity is a function of the varying delay time, and it yields T_1(H) or $T_{1\rho}$(H) as the exponential time constant. When phase domain sites are in the order of 10 nm or less, inter-domain spin diffusion averages out the T_1(H) of each different domain to one effective T_1(H) value. When the domains are greater than 50 nm, multiple T_1(H) and $T_{1\rho}$(H) are often observed. During the period of $T_{1\rho}$(H) relaxation, proton spin diffusion covers a distance of about 3 nm. If one effective $T_{1\rho}$(H) is observed and the intrinsic $T_{1\rho}$(H)s of the segments domains are different, it means that the domain size is below $1 \sim 3$ nm [20–25].

In this study, we used DSC, FTIR, and ^{13}C solid NMR techniques to study the miscibility of poly(ethyl oxazoline) (PEOx)/poly(4-vinylphenol) (PVPh) blends. PEOx is a tertiary amide amorphous polymer with a glass transition temperature (T_g) of 54°C. It has been reported that PEOx is miscible with a wide variety of other polymers [24,26–30]. This is attributed to the formation of strong interactions between hydroxyl groups and the amide carbonyl groups of PEOx. The structure of PVPh is similar to polystyrene, but it possesses a hydroxyl group attached to the aromatic ring, so that PVPh can act as a proton donor to form hydrogen bonds with other proton acceptor polymers. The PEOx/PVPh blends have been studied previously by means of DSC and FTIR [27]. In order to understand better the miscibility and the intimacy of mixing of PEOx /PVPh blends, high-resolution solid-state ^{13}C NMR was used in this study.

2. Experimental

2.1. Materials and preparation of blends

PEOx with a molecular weight of 500,000 and PVPh with a molecular weight of 22,000 were purchased from Polysciences, Inc. in Warrington, PA, USA. The PEOx/PVPh blends were prepared by solution casting from *N*,*N*-dimethylformamide (DMF) by slow evaporation at 60°C for one week; the residual solvent was removed under vacuum at 60°C for four weeks.

2.2. Differential scanning calorimeter

The calorimetric measurements were made on a Perkin-Elmer Pyris 1 differential scanning calorimeter under a dry nitrogen atmosphere. The instrument was calibrated with indium and zinc standards for low and high temperature regions, respectively. For both pure polymers and their blends, the samples were first scanned from 25 to 180°C at 20°C/min, followed by quenching to 25°C at a rate of 200°C/min and then scanned to 180°C at 20°C/min. The values of the T_g were taken as the midpoint of the heat capacity transition.

2.3. Fourier-transform infrared spectroscopy

FTIR spectra were obtained using a Bio-rad FTS6000 spectrometer. Thin films of the blends were cast on NaCl windows from 0.5% (w/v) DMF solutions. After most of the solvent was evaporated at room temperature, the films were transferred to a vacuum oven and were kept at 80°C for 2 weeks to remove residual solvent. All spectra were recorded at room temperature. A minimum of 128 scans at a resolution of 2 cm^{-1} was signal averaged. The films used in this study were sufficiently thin to obey the Beer–Lambert law.

2.4. Solid-state NMR

High-resolution solid-state NMR experiments were carried out at ambient temperature (27°C) on a JEOL JNM-EX400 FT NMR spectrometer at the resonance frequencies of 399.65 MHz for proton and 100.40 MHz for carbon. High-resolution ^{13}C NMR spectra were obtained using CP/MAS together with high-power DD. The 90° pulse width of 5.5 μs was employed with free induction decay (FID) signal accumulation. The CP Hartmann–Hahn contact time was set at 1.0 ms for all experiments; this was demonstrated to be the suitable time for detecting CP/MAS/DD NMR spectra for both the pure components and the blends. The rate of MAS was 5.0–5.4 kHz for measuring the ^{13}C spectra and the relaxation times. Total sideband suppression (TOSS) was used for suppressing the spinning side bands. The ^{13}C chemical shifts were calibrated by taking the ^{13}C chemical shift of the methine carbon of solid adamantine (29.5 ppm relative to TMS) as an external reference.

The proton spin–lattice relaxation times in the laboratory frame T_1(H) were measured, using the inversion-recovery (IR) method, by monitoring the decay of specific carbon peak intensities after a $\pi-\tau-\pi/2$ inversion-recovery pulse sequence followed by cross-polarization. The proton spin–lattice relaxation times in the rotating frame, $T_{1\rho}$(H), were determined by observing the carbon CP signal intensities following a variable ^{1}H spin-locking pulse.

Table 1
Glass transition temperature of PEOx, PVPh and their blends from DSC thermograms

Composition (PVPh) (wt%)	Glass transition (T_g) (°C)
0	54
10	61
30	80
50	96
70	100
90	135
100	157

3. Results and discussion

3.1. Differential scanning calorimetry

All the PEOx/PVPh blends were subject to DSC measurement for the purpose of examining microscopic miscibility. The T_g data of blends as a function of composition are summarized in Table 1. Each blend has a single glass transition temperature (T_g) that indicates the PEOx and PVPh can form miscible blends over the entire composition range. Fig. 1 shows the plot of T_g vs. composition, the T_gs of the blends are all below the average composition line. It has been generally suggested that the dependence of T_gs on the composition of the miscible polymer blends can be correlated by the following equation [31,32]:

$$T_g = \frac{w_A T_{gA} + K w_B T_{gB}}{w_A + k w_B}, \quad (1)$$

where w_A and w_B are the weight fractions of the components, T_{gA} and T_{gB} are the corresponding glass transition temperatures; and k and q are fitting constants. The solid curve in Fig. 1 is drawn using the equation with k value of 4 and q value of 82.

In general, the parameter q may be considered as a measure of the strength of the specific interactions in polymer blends [33]. When the interactions between chains of different polymers are weaker than those between chains of the same polymer q is negative; otherwise, q is positive. In this study, a positive q of 82 was obtained, which means that the intermolecular interactions between PEOx and PVPh might be strong, and the inter-molecular interactions were further investigated by FTIR as discussed next.

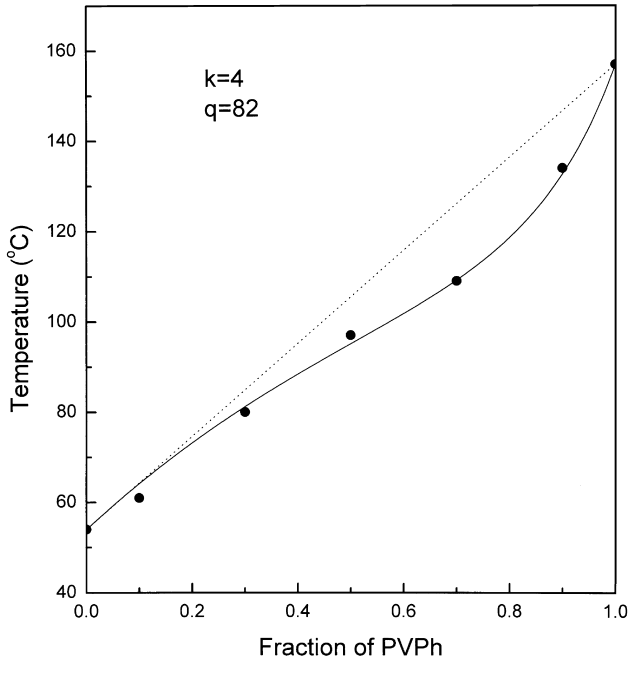

Fig. 1. Plot of glass transition temperature for PEOx/PVPh blends vs. weight fraction of PVPh. Solid dot (●) experimental data points; (—) curve fitting of Eq. (1) with $k = 4$ and $q = 82$.

3.2. Fourier transform infrared spectroscopy

Fig. 2 summarizes the stretching bands of the PEOx/PVPh blends at the region of 3000–3600 cm^{-1} extracted from the spectra of the FTIR measurements. Two vibration bands related to 'free' and intra-associated O–H groups appear in pure PVPh (curve A), at 3520 and 3358 cm^{-1}, respectively [34]. Free O–H groups refer to those hydrogen atoms that are not involved in hydrogen bonding. With the addition of PEOx in the blends, the band of the free OH groups becomes less and less detectable, indicating that an increasing number of hydroxyl groups are involved in the inter-molecular association with the carbonyl groups. Furthermore, the center of the broad hydrogen bonded band shifts gradually to lower frequency when the PEOx

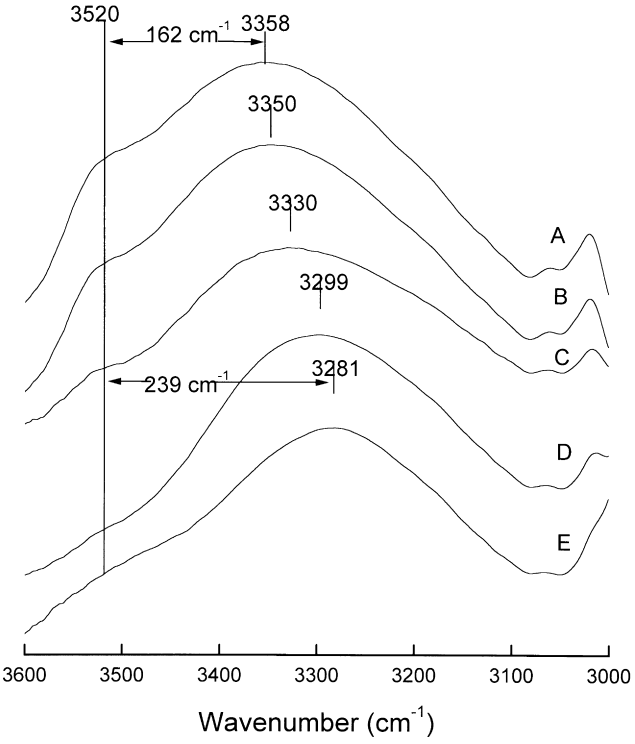

Fig. 2. FTIR spectra in the hydroxyl stretching region of the PEOx/PVPh blends: (A) 100; (B) 90; (C) 70; (D) 50; and (E) 30 wt% PVPh.

content in the blend increases. The frequency difference between the free hydroxyl groups and the hydrogen bonded hydroxyl groups can be used as a measure of the average strength of the intermolecular interactions [35]. In this study, it can be seen that the average strength of the hydrogen bond between the phenolic hydroxyl group in PVPh and the amide carbonyl group of PEOx ($\Delta\nu = 239\ cm^{-1}$ in curve E) is higher than that of the self-associated hydroxyl groups in PVPh ($\Delta\nu = 162\ cm^{-1}$ in curve A). The above results indicate that strong hydrogen bonding exists between PEOx and PVPh.

The FTIR spectra in the carbonyl stretching region for PEOx/PVPh blends are shown in Fig. 3. The two peaks at 1597 and 1611 cm^{-1} are related to the different C=C stretching vibrations of the benzene ring of PVPh. The intensity of these two peaks decreases as the PEOx content increases in the blends. The strong adsorption band of PEOx (curve A), centered at 1644 cm^{-1}, corresponds to amide carbonyl stretching [36]. As the PVPh content increases in the blends, the center of the amide carbonyl band shifts to lower frequency. It is well known that, when the double bond character of the carbonyl group becomes weaker the force constant of the bond becomes smaller, and the corresponding frequency occurs at lower frequency. These changes also support the idea that a strong hydrogen bond exists between the carbonyl groups of PEOx and the hydroxyl groups of PVPh.

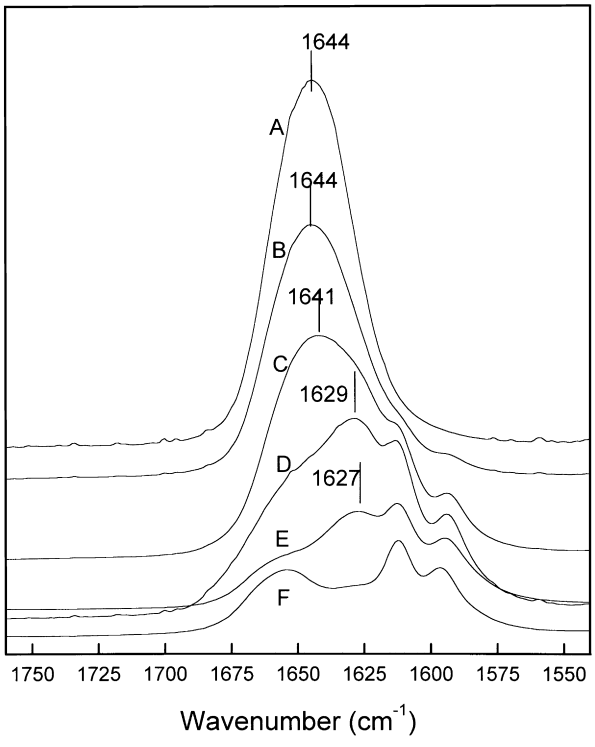

Fig. 3. FTIR spectra in the carbonyl stretching region of the PEOx/PVPh blends: (A) 100; (B) 90; (C) 70; (D) 50; (E) 30; and (F) 10 wt% PEOx.

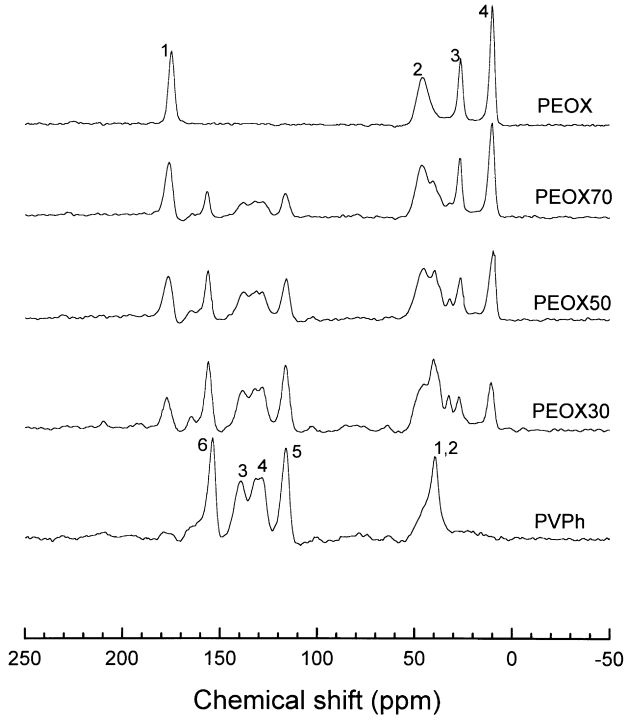

Fig. 4. ^{13}C CP/MAS/DD spectra of the PEOx/PVPh blends.

3.3. ^{13}C CP/MAS/DD solid-state NMR spectra

The ^{13}C CP/MAS/DD spectra of PEOx, PVPh, and their blends are shown in Fig. 4. Four peaks can be observed for pure PEOx. The resonance line at 174.7 ppm is for the carbonyl (C=O) carbon. The pure PVPh has six resonance lines and the resonance line at 153.8 ppm corresponds to the hydroxyl-substituted carbon (C-6). All other line assignments are given in Fig. 4 as assigned below [24,37].

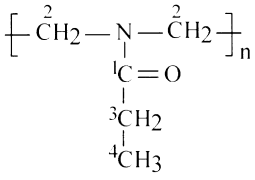

(PEOx)

(PVPh)

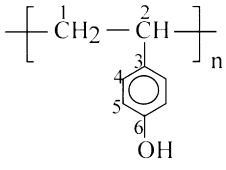

Table 2 lists the resonance peak positions for the blends

Table 2
Chemical shift of the ^{13}C CP/MAS/DD spectra of PEOx, PVPh and their blends (ppm)

Composition (PEOx wt%)	PEOx	PVPh				PEOx	PVPh	PEOx	
	C-1	C-6	C-3	C-4	C-5	C-2	C-1, 2	C-3	C-4
0		153.8	139.3	128.5	116.3		39.7		
30	176.9	155.7	138.4	127.9	116	43.7	39.8	26.7	10.2
50	176.6	156.3	137.8	131.4	116	45.5	40.2	26.8	10.3
70	175.6	156.3	137.6	126.7	116	46.1	40.3	26.9	10.2
100	174.7					45.8		26.4	10.2

and for the pure components. The chemical shifts of the carbonyl carbon (C=O) of PEOx and the hydroxyl-substituted carbon of PVPh change monotonously with composition (Fig. 5). The variation in chemical shift indicates intermolecular interactions between the two components. It is well known that specific interactions among polymer chains will change the chemical environment of the neighboring molecules, which can cause changes of magnetic shielding and hence the chemical shift [12,38–41]. From Table 2, it can be seen that the carbonyl carbon peak of PEOx shifts downfield as the amount of PVPh increases in the blends. A downfield shift of 2.2 ppm can be observed for the PEOx30/PVPh70 blend relative to the pure PEOx. A Similar shift can be observed for the hydroxyl-substituted carbon of PVPh, which shifts downfield with increasing PEOx concentration. A downfield shift of 2.7 ppm was observed when the concentration of PEOx increased to 70% (w/w) relative to the pure PVPh. Such downfield shifts are indicative of strong intermolecular hydrogen-bonding between PEOx and PVPh segments, consistent with the DSC and FTIR results [20,24].

3.4. Proton spin–lattice relaxation time

To obtain more detailed information about the scale of miscibility and phase structure of the PEOx/PVPh blends, dynamic relaxation experiments were conducted, which include the measurements of the spin–lattice relaxation time in the laboratory frame T_1 (H), and in the rotating frame $T_{1\rho}$(H). In T_1 (H) experiment, peak intensities of PEOx, PVPh and their blends change exponentially as a function of delay time (τ) and the T_1 (H) values can be calculated using Eq. (2)

$$\mathrm{Ln}\,[M_e - M_\tau)/(2M_e) = -\tau/T_1(\mathrm{H}), \quad (2)$$

where T_1 (H) is the proton spin–lattice time in the laboratory frame, τ is the delay time used in the experiment, M_τ is the corresponding peak intensity, and M_e is the intensity of the

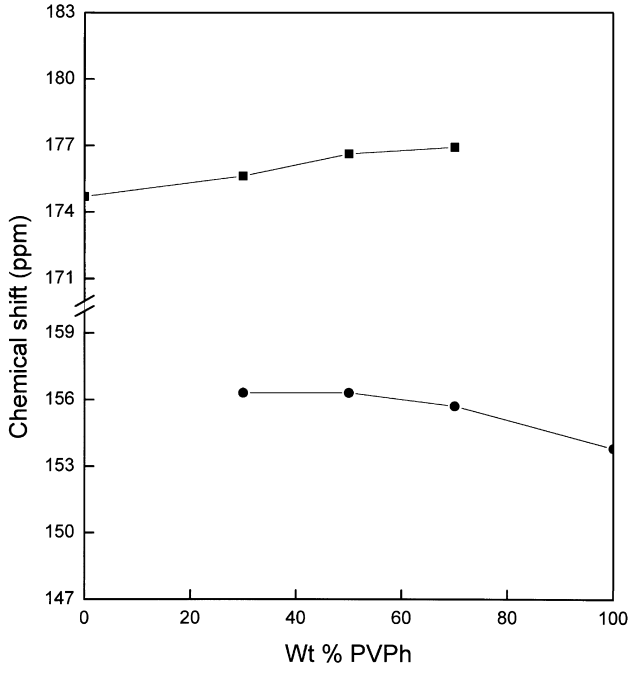

Fig. 5. Composition dependence of the chemical shifts of the carbonyl group (■) the hydroxyl-substituted carbon (●) resonance in the PEOx/PVPh blends.

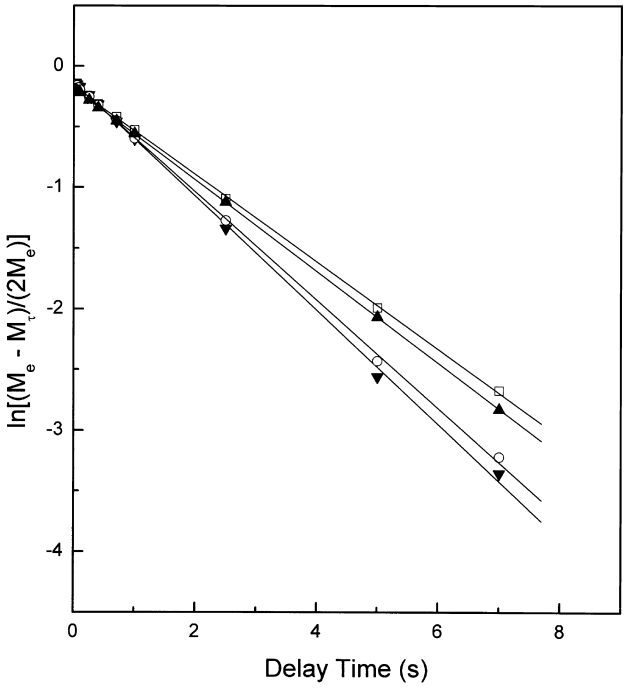

Fig. 6. Logarithmic plot of resonance intensity (at 46 ppm) vs. delay time to measure T_1(H). PEOx/PVPh: (□) 100/0, (▲) 70/30, (○) 50/50, (▼) 30/70.

Table 3
T_1 (H) values (s) for PEOx, PVPh and their blends (the accuracy of the measurements is ±5%)

Composition	PEOx C-3	PVPh C-5
0	–	1.32
30	2.04	2.17
50	2.39	2.35
70	2.62	2.65
100	2.76	–

resonance at $\tau \geq 5\ T_1$ (H). By plotting ln $[(M_e - M_\tau)/(2M_e)]$ against τ, T_1 (H) can be obtained from the slope of such a plot.

The plots of $\ln[(M_e - M_\tau)/(2M_e)]$ vs. τ for the selected carbon (PEOx C-2) are shown in Fig. 6. It can be seen that all the T_1 (H) values were found to be single-exponential. From the slopes of the plots, T_1 (H)s were obtained, and the results of T_1 (H) for PEOx, PVPh and their blends are summarized in Table 3. Intermediate values of T_1 (H) were obtained for the blends compared to those of the two pure components. These results indicate that fast spin diffusion occurred among all the protons in these blends, which averages out the entire relaxation process. Therefore, the blends are homogenous on the scale where the spin diffusion occurs within the time-frame of T_1 (H), and the mixing scale can be estimated using the one-dimensional diffusion equation for the average diffusive path length [42–44]:

$$\langle L^2 \rangle = (6DT_i), \tag{3}$$

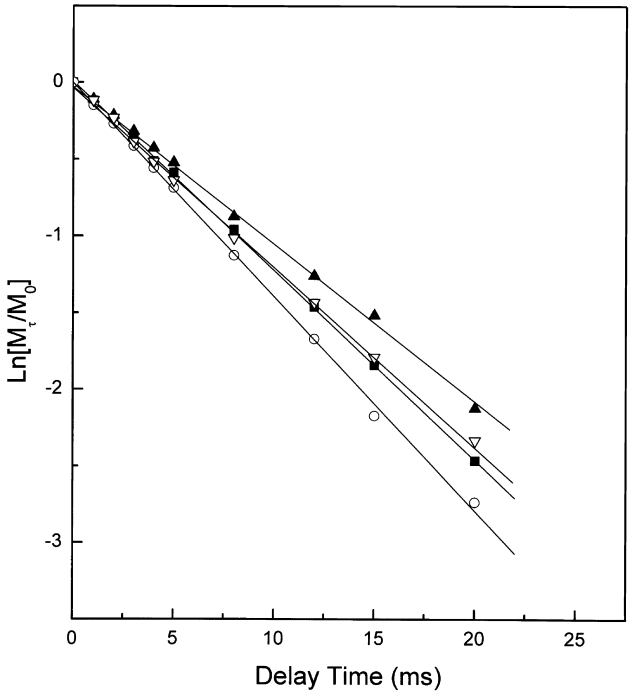

Fig. 7. Logarithmic plot of resonance intensity of PEOx C-2 vs. delay time to measure $T_{1\rho}$ (H). PEOx/PVPh: (○) 100/0, (▽) 70/30, (▲) 50/50, (■) 30/70.

where D is the spin-diffusion coefficient, which depends on the average proton to proton distance as well as dipolar interaction. It has a typical value in the order of $4 \sim 6 \times 10^{-16}$ $m^2 s^{-1}$. T_i is the relaxation time, T_1 (H) or $T_{1\rho}$ (H), according to the relaxation experiment. On the basis of T_1 (H), it is believed that the two polymers are intimately mixed on a scale of less than 100 nm. Since such mixing level reflects the sum of domain A plus domain B of the blends, the domain size of a constituent domain is less than 50 nm.

The spin–lattice relaxation time in the rotating frame $T_{1\rho}$ (H) was measured to examine homogeneity of the PEOx/PVPh blends at the molecular level. In this measurement, the intensities of carbon peaks of PEOx, PVPh and their blends display single exponential decays as a function of delay time, and the $T_{1\rho}$ (H) values were calculated according to the exponential function model:

$$M_\tau = M_0 \exp[-\tau/T_{1\rho}(\mathrm{H})]. \tag{4}$$

Rearranging Eq. (4) and taking the nature logarithm, we have:

$$\ln(M_\tau/M_0) = -\tau/T_{1\rho}(\mathrm{H}). \tag{5}$$

Fig. 7 shows the plots of $\ln(M_\tau/M_0)$ vs. spin-locking time τ for the selected carbons (PEOx C-2), which gives single exponential decays. Values of calculated $T_{1\rho}$ (H) are summarized in Table 4. A single $T_{1\rho}$ (H) value was obtained for both pure components and blends and values of the blends were larger than those of the two pure components, indicating strong hydrogen bonding between the two components, that restricts the segmental motion of the polymer chains and cause the relaxation times of the blends to be longer than those of the pure components [24,37,45]. Thus, the blends are homogeneous on the $T_{1\rho}$ (H) sensitive scale of 2–3 nm according to Eq. (3).

4. Conclusions

A 2.2 ppm downfield shift for the carbonyl group of PEOx was observed when the PVPh concentration was 70 wt% in the blend; and a 2.7 ppm downfield shift for the hydroxyl-substituted carbon of PVPh was observed when the PVPh concentration was 30 wt% in the blend consistent with the formation of strong hydrogen bonds between the two components. The T_1 (H) results were in good agreement

Table 4
$T_{1\rho}$ (*H*) values (ms) for PEOx, PVPh and their blends (the accuracy of the measurements is ±5%)

Composition (PEOx wt%)	PEOx C-3	PVPh C-5
0	–	6.79
30	8.59	8.10
50	8.74	8.90
70	8.57	8.06
100	7.16	–

with the thermal analysis and FTIR results. The blending of PEOx and PVPh restricts the segmental motional of the polymer chains because the $T_{1\rho}$ (H) values of the blends are longer than those of the pure components.

Acknowledgements

Partial financial support of the grant RGC HKUST 6120/99P is acknowledged.

References

[1] Srinivasan D, Natarajan TS, Rangarajan G, Bhat SV, Wessling B. Solid State Commun 1999;110:503–8.
[2] Baik Doo Hyun, Kim Gil Lae, Park Yun Heum, Lee Youngkwan, Son Yongkeun. Polym Bull (Berlin) 1998;41:713–9.
[3] Olabisi O, Robeson LM, Shaw MT. Polymer–polymer miscibility. New York: Academic Press, 1979.
[4] Shaw MT. Polymer blends and mixtures. In: Walsh DJ, Higgins JS, Maconnachie A, editors. NATO, Advanced Study Institute Series E89. Boston, MA: Martinus Nijhoff Publishers, 1985.
[5] Walsh DJ, Rostami S. Adv Polym Sci 1985;70:119.
[6] Ultracki LA. Polymer alloy and blends. Munich: Hanser Publishers, 1989.
[7] Kaplan DS. J Appl Polym Sci 1976;20:2615.
[8] Coleman MM, Graf JF, Painter PC. Specific interaction and the miscibility of polymer blends. Lancaster, PA: Technomic Publishing Inc, 1991.
[9] Mcbrierty VJ, Packer KJ. Nuclear magnetic resonance in solid polymer. Cambridge, UK: Cambridge University Press, 1993.
[10] Mathias LJ, editor. Solid state NMR of polymer. New York: Plenum Press, 1991.
[11] Saxena S, Cizmeciyan D, Kornfield JA. Solid State Nucl Mag Reson 1998;12:165–81.
[12] Zhang X, Takegoshi K, Hikichi K. Polymer 1992;33:712.
[13] Qin C, Priesm ATN, Belfiore LA. Polym Commun 1990;31:177.
[14] Miyoshi T, Takegoshi K, Hikichi K. Polymer 1997;38:2315.
[15] McBrierty VJ, Douglass DC, Kwei TW. Macromolecules 1978;11:1265.
[16] Stejskal EO, Schaefer J, Sefcik MD, Mckay R. Macromolecules 1981;14:275.
[17] Caravatti P, Deli JA, Bodenhausen G, Ernst RR. J Am Chem Soc 1982;104:5506.
[18] Veeman WS, Maas WEJR,. In: Blumich B, editor. Solid-state NMR III: organic matter. Berlin: Springer, 1994.
[19] Michel D, Engelke F. In: Blumich B, editor. Solid-state NMR III: organic matter. Berlin: Springer, 1994.
[20] Zheng S, Guo Q, Mi Y. J. Polym Sci, Part B: Polym Phys 1998;36:2291–300.
[21] Zhong Z, Guo Q, Mi Y. Polymer 1998;40:27–33.
[22] Cheung MK, Zheng S, Mi Y, Guo Q. Polymer 1998;39:6289–92.
[23] Zhong Z, Zheng S, Mi Y. Polymer 1999;40:3829–34.
[24] Lau C, Zheng S, Zhong Z, Mi Y. Macromolecules 1998;31:7291–7.
[25] Zhong Z, Mi Y. J Polym Sci, Part B: Polym Phys 1999;37:237–45.
[26] Meaurio O, Cesteros LC, Katime I. Macromolecules 1996;29:4598.
[27] Wang LF, Pearce EM, Kwei TK. J Polym Sci, Part B: Polym Phys 1991;29:619.
[28] Dai J, Goh SH, Lee SY, Siow KS. J Appl Polym Sci 1994;53:837.
[29] Dai J, Goh SH, Lee SY, Siow KS. Polymer 1995;35:2174.
[30] Parada LG, Meaurio E, Katime I. Macromol Chem Phys 1998;199:1597–602.
[31] Kwei TK, Pearce EM, Pennacchia CM. Macromolecules 1987;20:174.
[32] McBrierty VJ, Douglass DC. Phys Rep 1980;63:61.
[33] Kwei TK. J Polym Sci, Polym Lett Ed 1984;22:307.
[34] Dong J, Ozaki Y. Macromolecules 1997;30:286–92.
[35] Dai Jie, Goh SH, Lee SY, Siow KS. Polymer 1996;37:3259–64.
[36] Goh SH, Lee SY, Zhou X, Tan KL. Polymer 1999;40:2667–73.
[37] Jack KS, Whittaker AK. Macromolecules 1997;30:3560–8.
[38] Grobelny J, Rice DM, Karasez FE, Macknight WJ. Macromolecules 1990;23:177.
[39] Qin C, Pries ATN, Belfiore LA. Polym Commun 1990;31:177.
[40] Zhang X, Takegoshi K, Hikichi K. Macromolecules 1992;25:2336.
[41] Zhang X, Solomon DH. Macromolecules 1994;27:4919.
[42] McBrierty VJ, Douglass DC. J Polym Sci Macromol Rev 1981;16:295.
[43] Demco DE, Johannsson A, Tegenfeldt J. J Solid State Nucl Magn Reson 1995;4:13.
[44] Clauss J, Schmidr-Rohr K, Spiess HW. Acta Polym 1993;44:1.
[45] VanderHart DL, Garroway AN. J Chem Phys 1979;71:2773.